15th World Congress on Computational Mechanics (WCCM-XV)
8th Asian Pacific Congress on Computational Mechanics (APCOM-VIII)
Virtual Congress: 31 July – 5 August 2022
S. Koshizuka (Ed.)

REPRODUCTION METHOD OF MECHANICAL ANISOTROPY INDUCED BY ROLLING IN CRYSTAL PLASTICITY FE SIMULATION

YUSUKE YAGINUMA[1] AND YOSHITERU AOYAGI[2]

[1] Department of Finemechanics, Tohoku University
6-6-01 Aramaki Aoba, Aoba-ku, Sendai, 980-8579, JAPAN
yuusuke.yaginuma.s6@dc.tohoku.ac.jp

[2] Department of Finemechanics, Tohoku University
6-6-01 Aramaki Aoba, Aoba-ku, Sendai, 980-8579, JAPAN
aoyagi@tohoku.ac.jp (https://web.tohoku.ac.jp/aoyagi/)

Key words: High Entropy Alloys, Crystal Plasticity, Finite Element Analysis, Rolling Texture, Mechanical Anisotropy

Abstract. *In this study, we investigate a method for accurately representing mechanical anisotropy in a crystal plasticity finite element (FE) analysis using a computational model with a small number of crystal grains to reproduce the rolling texture. We propose a method for extracting the preferred orientation of the rolling texture, construct a computational model using this method, and perform a crystal plasticity FE simulation.*

1 INTRODUCTION

The crystal plasticity finite element (FE) analysis considering the microscopic information describes the mechanical response of polycrystalline metals at the grain level. When the crystal orientation information of the actual material is applied to the computational model for the crystal plasticity FE simulation, the crystal orientation is often randomly extracted from the electron backscatter diffraction pattern (EBSD) measurement data [1]. The number of crystal grains in crystal plasticity FE analysis is limited to a small number compared to the actual crystalline metals due to the calculation cost. When the number of crystal grains in a computational model is small, the conventional method of randomly extracting crystal orientations from EBSD measurement data and reflecting them in the computational model may result in different analytical results among different models due to the combination of crystal orientations. As a result, there may be a problem of not obtaining appropriate analysis results. If the crystal orientation distribution of the actual material can be reproduced by a computational model with a small number of grains, the computational cost can be reduced. The rolling texture induced by the rolling process significantly affects the mechanical properties of rolled metals, and the rolling texture causes mechanical anisotropy [2]. Numerical reproduction of the rolling texture of the actual material reproduces the mechanical anisotropy of rolled metals in a crystal plasticity FE analysis.

This study investigates a method to reproduce mechanical anisotropy by accurately

reflecting the rolling texture in a computational model with a small number of grains for crystal plasticity FE simulation. We propose a method to extract the crystal orientation representative of the rolling texture from the crystal orientation measured by EBSD and reflect it in the computational model. The computational model with the crystal orientation determined by the proposed method was prepared, and a crystal plasticity FE simulation was performed. Based on the obtained results, the variability of the numerical results and the reproducibility of mechanical anisotropy by the proposed method were evaluated in comparison with the conventional method.

2 ANALYSIS AND ORIENTATION EXTRACTION METHOD

2.1 Crystal plasticity finite element analysis

For the elasto-viscoplastic constitutive equation in crystal plasticity theory, we used the equation proposed by Peirce et al. [3].

$$\overset{\nabla}{\boldsymbol{T}} = \boldsymbol{C}^e : \boldsymbol{D} - \boldsymbol{C}^e : \sum_{\alpha} (\boldsymbol{s}^{(\alpha)} \otimes \boldsymbol{m}^{(\alpha)})_s \dot{\gamma}^{(\alpha)} \tag{1}$$

where $\overset{\nabla}{\boldsymbol{T}}$ is the co-rotational rate of Cauchy stress, C^e is the anisotropic modulus tensor, $\boldsymbol{D}$ is the deformation rate tensor, $\boldsymbol{s}^{(\alpha)}$ is the slip direction vector, $\boldsymbol{m}^{(\alpha)}$ is the normal vector of the slip plane, $(\ )_x$ is the symmetric part of the second-order tensor, and $\dot{\gamma}^{(\alpha)}$ is the slip rate. For the slip rate in the elasto-viscoplastic constitutive equation, the following Pan-Rice type slip rate hardening law [4] is used.

$$\dot{\gamma}^{(\alpha)} = \dot{\gamma}_0^{(\alpha)} \left(\frac{\tau^{(\alpha)}}{g^{(\alpha)}} \right) \left| \frac{\tau^{(\alpha)}}{g^{(\alpha)}} \right|^{\frac{1}{m}-1} \tag{2}$$

where $\dot{\gamma}_0^{(\alpha)}$ is the reference slip rate, $\tau^{(\alpha)}$ is the resolved shear stress, $g^{(\alpha)}$ is the flow stress, and m is the strain rate sensitivity. The flow stress is expressed as

$$g^{(\alpha)} = \tau_0^{(\alpha)} + \sum_{\beta} a \mu \tilde{b} \sqrt{\Omega^{(\alpha\beta)} \rho_d^{(\beta)} + \Omega_{GN}^{(\alpha\beta)} \rho_{GN}^{(\beta)}} \tag{3}$$

where $\tau_0^{(\alpha)}$ is the reference value of the flow stress, a is a numerical constant, μ is the shear modulus, $\tilde{b}$ is the magnitude of the Burgers vector, $\rho_d^{(\beta)}$ and $\rho_{GN}^{(\beta)}$ $\rho_{GN}^{(\beta)}$ are respectively the SS and GN dislocation densities, and $\Omega^{(\alpha\beta)}$ and $\Omega_{GN}^{(\alpha\beta)}$ are matrices representing the interaction of the SS and GN dislocations, respectively.

2.2 Orientation extraction method

In this study, we propose the following method: weights are assigned to the crystal orientation of each measurement point measured by EBSD as an index of orientation, and the crystal orientation is extracted based on these weights and applied to the computational model. Figure 1 shows the (111) pole figure and EBSD observations of 20 % asrolled FeMnNiCoCr alloy without heat treatment.

At first, the misorientation angle between a measurement point in the EBSD measurement data and other measurement points is calculated. The number of measurement points with an

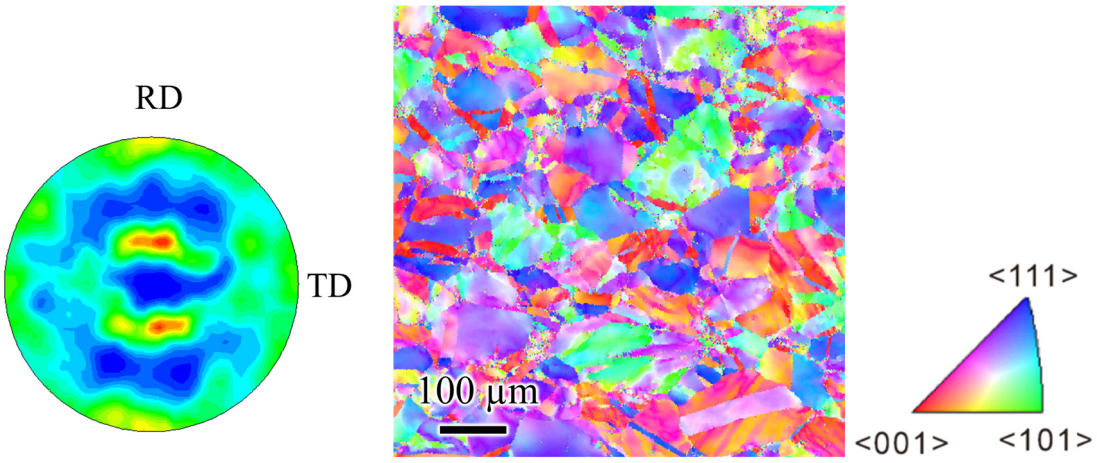

(a) (111) Pole figure. (b) EBSD measurement result.

Figure 1: (111) pole figure and EBSD observations of the a rolled FeMnNiCoCr alloy.

orientation difference below a threshold value is assigned as the weight of the measurement point. Here, we call the threshold value the misorientation angle for the weights. This operation assigns weights to the crystal orientation of all measurement points in the EBSD data. The weighted crystal orientations are arranged in order of increasing weight. The crystal orientation is randomly extracted from the top x % in order of weight and applied to the computational model.

3 ANALYSIS MODELS AND ANALYSIS RESULT

3.1 Identification of material constants

Although microstructural observation has become easier with the development of the EBSD method, a wealth of knowledge and experience is required to understand the phenomena inside

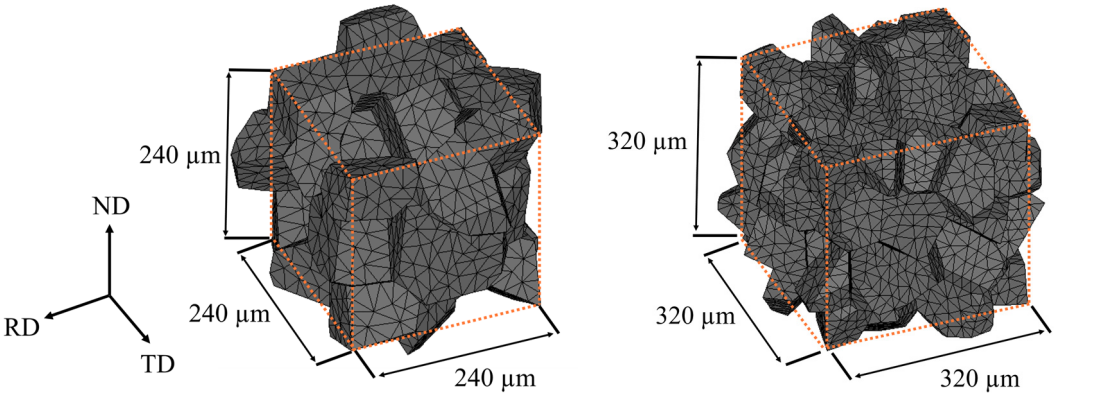

(a) Computational model of 27 grains. (b) Computational model of 64 grains.

Figure 2: Computational models.

materials correctly. In addition, dynamic observation of changes in dislocation density and crystal orientation requires testing inside the SEM equipment, which is extremely difficult due to the limited size of the specimen. In this study, material parameters were identified by curve fitting the true stress-strain curve obtained by numerical analysis, so that the curve shows the same trend as the true stress-strain curve obtained by uniaxial tensile test in the region below about 0.02 strain. We used a computational model of 729 grains whose crystal orientation was

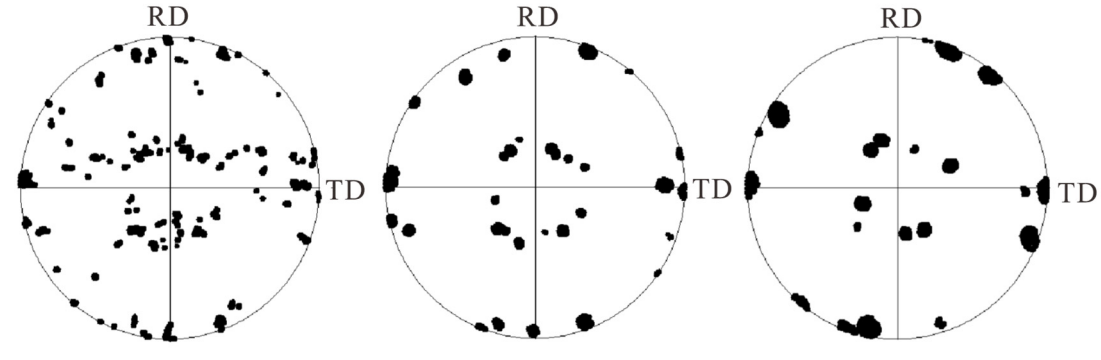

(1) 1 ° (2) 4 ° (3) 7 °°

(a) Extracted from top 3 %.

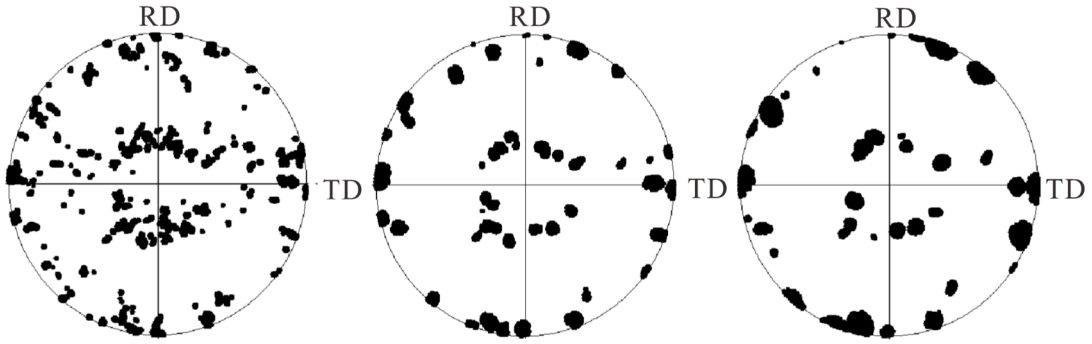

(1) 1 ° (2) 4 ° (3) 7 °

(b) Extracted from top 6 %.

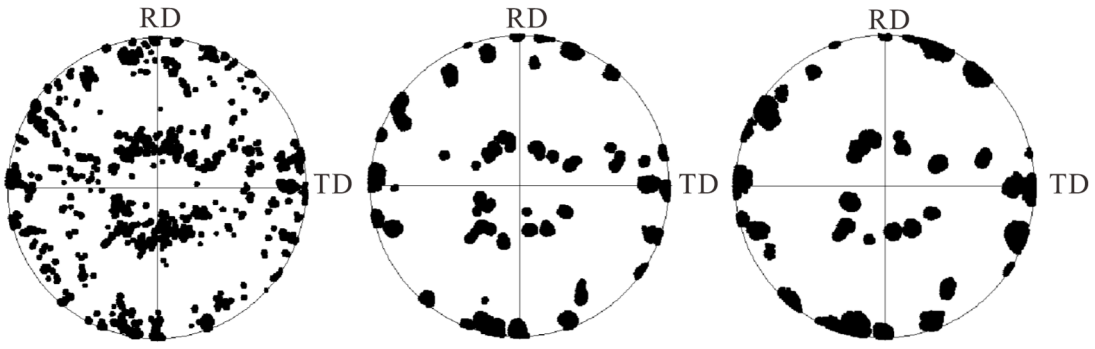

(1) 1 ° (2) 4 ° (3) 7 °

(c) Extracted from top 9 %.

Figure 3: (111) pole figure of crystal orientation extracted by the proposed method.

randomly determined from EBSD measurement data. The anisotropic elastic moduli C_{11}, C_{12}, C_{44} and the magnitude of the Burgers vector $\tilde{b}$ are literature values [5~8]. The initial dislocation density $\rho_d^{(\beta)}$, dislocation annihilation rate k, and accumulated dislocation length r were identified by fitting the stress-strain curve, and their values are as follows: $\rho_d^{(\beta)} = 2.5 \times 10^{14}$ m^{-2}, $k = 4.0 \times 10^{-15}$ m^2, $r = 50.0$ nm.

3.2 Analysis model

The simulation assuming a rolled FeMnNiCoCr alloy whose average grain size is 80 μm was performed. Two types of computational models with a different number of grains were prepared, i.e., 27 grains (16,029 first-order tetrahedron elements) and 64 grains (46,643 elements). As shown Fig. 2, the coordinate axes of the computational model correspond to the rolling direction (RD), transverse direction (TD), and normal direction (ND), and periodic boundary condition is applied in all directions. The tensile loading direction is RD or transverse direction (TD). To compare the proposed method with a method in which orientation is randomly extracted from all EBSD measurement data (the conventional method), we applied the crystal orientation given by the proposed and conventional methods to the above computational models.

Crystal orientation is extracted from the top 3, 6, or 9 % in the weighted order as applied crystal orientation to the computational models. The misorientation angle for the weights was set to 1, 4, or 7°. Figure 3 shows the (111) pole figures plotted by the crystal orientation

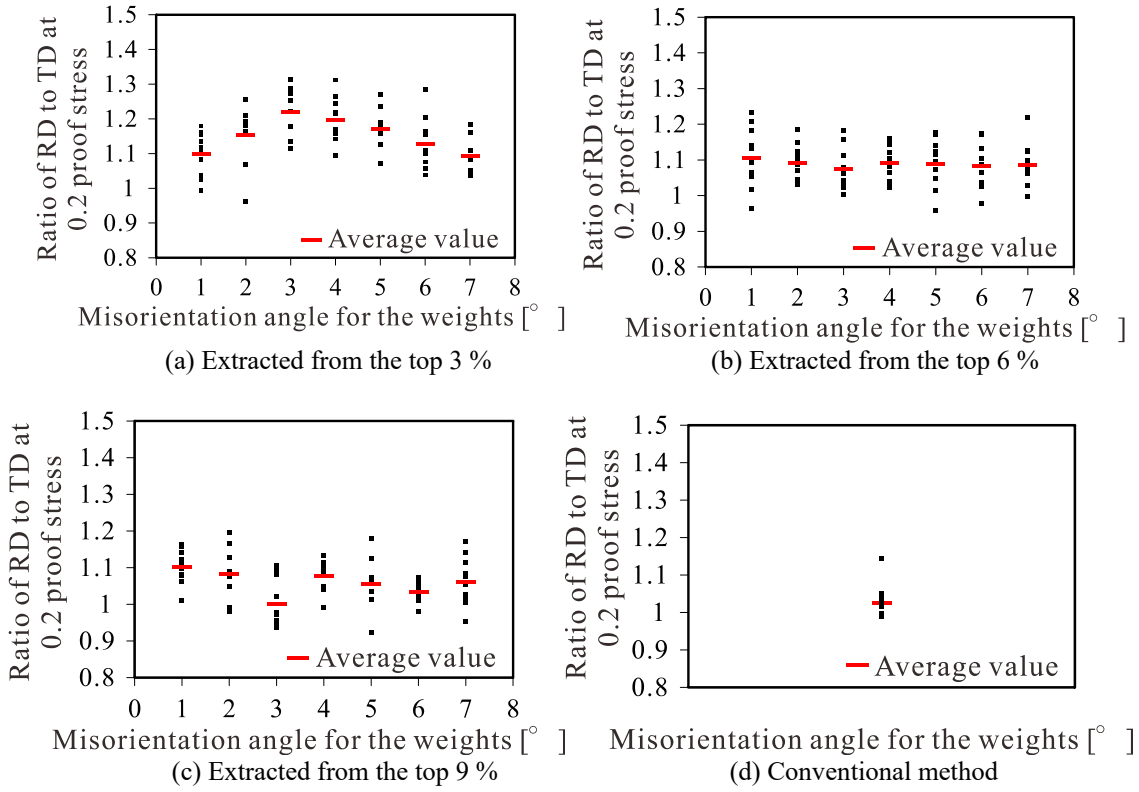

Figure 4: Meachanical anisotropy obtained from the models of 27 grains.

extracted by each condition. Ten different combinations of crystal orientation are applied to the computational modes to investigate the dispersion of calculated results due to random extraction. In this analysis, the number of EBSD measurement points is 108,580, which excludes those with a CI value of 0.5 or less. The number of crystal orientation data extracted from the top 3, 6, and 9 % in order of weight is 3,257, 6,515, and 9,772, respectively. It was confirmed that the larger the misorientation angle for the weights, the more localized the extracted orientation becomes. The variation of 0.2 % proof stress and mechanical anisotropy (ratio of 0.2 % proof stress of RD to TR) obtained analysis results were investigated.

3.3 Analysis Results

Figures 4 and 5 show the analysis results for the model of 27 and 64 grains, respectively. The ten results obtained by different combinations of crystal orientation are plotted in (a)~(c) for each top percentage in order of weight, with the horizontal axis representing the misorientation angle for the weights and the vertical axis representing the ratio of 0.2 % proof stress (TD/RD). Figures 4(d) and 5(d) are the simulation results calculated by the conventional method. The ratio of 0.2 % proof stress obtained by the uniaxial tensile test is 1.11. The dispersion of the results is observed for both the 27-grain and 64-grain models, suggesting that a computational model with a larger number of grains would be necessary to reduce the dispersion and obtain a single result. The average values of both results obtained by the 27-grain and 64-grain models show larger mechanical anisotropy than those obtained with the

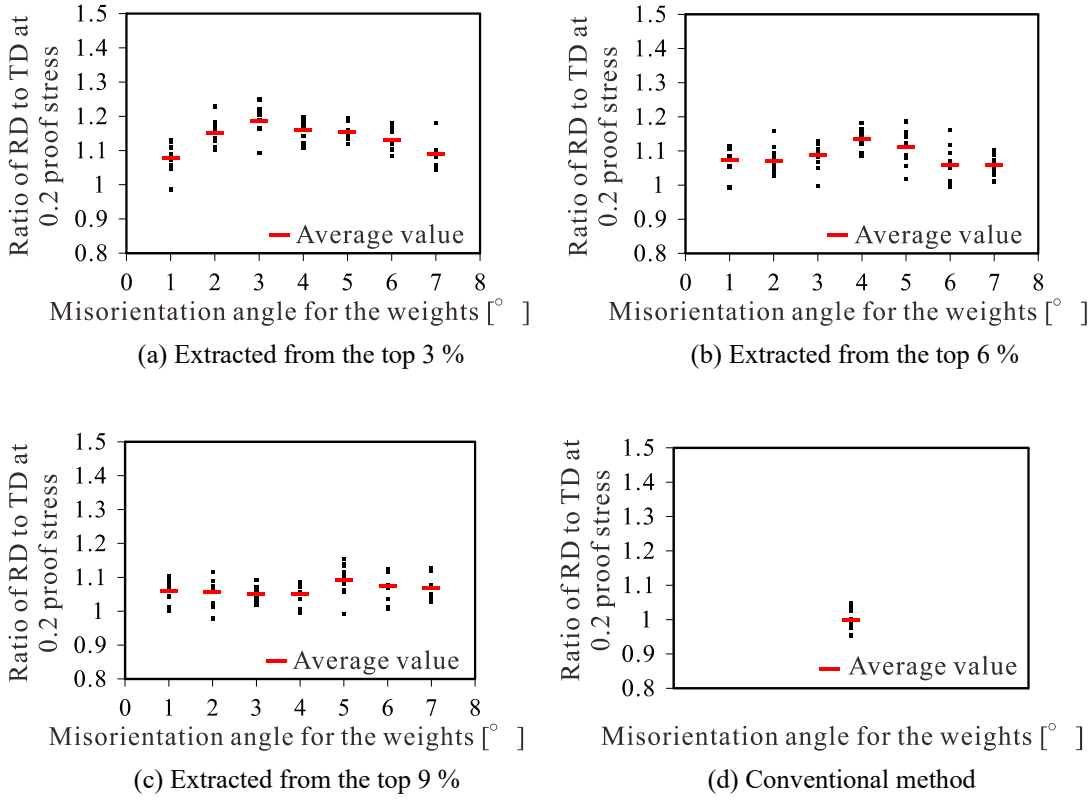

Figure 5: Meachanical anisotropy obtained from the models of 64 grains.

conventional method. A similar trend is observed for the results obtained by the 27-grain and 64-grain models when the crystal orientations are extracted from the top 3 % and 6 %. In the simulation with crystal orientations extracted from the top 3 %, the anisotropy peak is the largest when the misorientation angle for the weights is 3°. When crystal orientations are extracted from the top 6 %, there is no difference in anisotropy due to the misorientation angle for the weights. From the (111) pole figure in Fig. 3, it can be seen that the pole figure around the circumference of the crystal changed more significantly with the change in the misorientation angle for the weights from the top 3 %. This trend is thought to be because the number of crystal orientation data is too small when the data is extracted from the top 3 %, which is strongly affected by the misorientation angle for the weights. In the result calculated with the crystal orientations extracted from the top 9 %, a different trend is observed in the analytical results of the 27-grain and 64-grain computational models. In the 64-grain computational model, the anisotropy does not vary much with the misorientation angle for the weights, whereas in the 27-grain model, it varied more. Since the number of crystal orientation data from the top 9 % is larger than that from the top 3 and 6 %, the combinations number of crystal orientations increases, resulting in the dispersion in the average value in the 27-grain model. No dispersion is observed in the 64-grain computational model, but when orientations are extracted from the top 9%, the dispersion of anisotropy is likely to be greater. Based on the above, extracting the orientation from the top roughly 6 % in the weight order is considered necessary to reproduce the mechanical anisotropy of the materials used in this study.

4 CONCLUSIONS

In this study, we proposed a method to extract the preferential orientation of the rolling texture and reflect it in a computational model. A computational model was created using the proposed method, and a crystal plasticity finite element analysis was performed. The obtained results suggest that a computational model with a larger number of grains is necessary to reduce the variation and obtain a single result. When the crystal orientations were extracted from the top 6 % in the weight order, the mechanical anisotropy was close to the experimental value, independent of the difference in the misorientation angle for the weights. It is suggested that the orientation should be extracted from the top roughly 6 % of the weights to reproduce the mechanical anisotropy of the material studied in this research.

ACKNOWLEDGMENTS

This work was performed with the support of JSPS KAKENHI Grant Number 18H05453, 21K03745.

REFERENCES

[1] Aoyagi, Y., Crystal plasticity simulation of macroscopic yielding behavior of ultrafine-grained aluminum, *Transactions of JSME*, (2016) **82**, 15-00396.
[2] Nagashima, S., Texture and Anisotropy in Metallic Materials, *Materials Transactions,* (1983) **358**, 705-715.
[3] Peirce, D., Asaro, R. J. and Needleman, A., Material rate dependence and localized deformation in crystalline solids, *Acta Metallurgica*, (1983) **31**, 1951–1976.
[4] Pan, J. and Rice, J. R., Rate sensitivity of plastic flow and implications for yield-surface

vertices. *International Journal of Solids and Structures*, (1983) **19**, 973–987.
[5] Tanaka, K., Teramoto, T., and Ito, R., Monocrystalline elastic constants of fcc-crmnfeconi high entropy alloy. *MRS Advances*, (2017) **27**, 1429–1434.
[6] Li, X., Irving, D.L. and Vitos, L., First-principles investigation of the micromechanical properties of fcc-hcp polymorphic high-entropy alloys. *SCIENTIFIC REPORTS*, (2018) **8**, 1–8.
[7] Moon, J., Hong, S.L., Bae, J.W., Jang, M.J., Yim, D. and Kim, H.S., On the strain rate-dependent deformation mechanism of cocrfemnni high-entropy alloy at liquid nitrogen temperature. *Material Research Letters*, (2017) **5**, 472–477.
[8] Laplanche, G., Gadaud, P., Horst, O., Otto, F., Eggeler, G. and George, E.P., Temperature dependencies of the elastic moduli and thermal expansion coefficient of an equiatomic,single-phase cocrfemnni high-entropy alloy. *Journal of Alloys and Compounds*, (2015) **623**, 348–353.